

---

**METAL INDUCED CONFORMATIONAL CHANGES OF PRION PROTEIN INTO B-SHEET ISOFORMS SIMILAR TO AMYLOID**

---

**ONWUBIKO, Henry Amaechi**

Department of Biochemistry, University of Nigeria, Nsukka, Enugu State, Nigeria.

Email: [obinnaya4all@yahoo.com](mailto:obinnaya4all@yahoo.com) Phone: +234 8103918230

---

**ABSTRACT**

*The transmissible spongiform encephalopathies (TSEs) are characterized by the conversion of the normal cellular prion protein to its abnormal pathogenic isoform which has an increased beta-sheet structure, an increased absorbance at the 700nm region and an enhanced capacity to form amyloids. Investigation on metal induced structural perturbation in selected prion protein peptide from hamster, mouse and humans had residues of 23 – 231, 23 – 144, 23 – 106 and 90 – 231 in non-fibrillar versus amyloid isoforms analyzed with UV-visible scanning and Fourier transform infrared spectroscopy. The proteinase K resistant amyloid fragment (residues 90 – 231) exhibited a markedly high, broad absorbance at the 700nm region and an increase in beta-sheet character. Addition of copper to the corresponding non-fibrillar 90 – 231 peptides also markedly increased the absorbance of this segment at the 700nm region, and led to an infrared shifted reflecting an increase in beta-sheet secondary structure similar to that of the amyloid. The copper-prompted increase in beta sheet structure and induced enhancement of the absorbance at the 70nm region when added to the monomeric isoform similar to the amyloid suggest the importance of this structure in the determination of amyloid nucleation, stabilization, formation and perhaps prion infectivity.*

**Keywords:** Metals, Induced conformational changes, Prion protein, B-sheet isoforms, Amyloid

---

**INTRODUCTION**

Transmissible spongiform encephalopathies (TSEs) are a group of neurodegenerative infectious diseases which in humans include Kuru, Creutzfeld-Jakob disease, fatal familial insomnia, and Gerstmann-Straussler-Scheinker syndrome (William and Miller, 2002). It also includes bovine spongiform encephalopathy in cattle, chronic wasting disease in the North American deer and elk, and scrapie in sheep and goats (William and Miller, 2002).

In every case the main causative agent is the misfolded isoform of the normal cellular membrane glycoprotein known as prion protein or PrP<sup>C</sup> (Callahan *et al.*, 2001). PrP<sup>C</sup> is anchored to the plasma membrane by a glycosyl-phosphatidyl inositol which is thought to

enhance the infectivity of the disease causing isoform PrP<sup>SC</sup> (Borchelt *et al.*, 1993). PrP<sup>SC</sup> differs from normal cellular isoform PrP<sup>C</sup> by its higher beta sheet content and lower alpha helical secondary structure resulting in its generally increased resistance to proteinase K catalyzed cleavage (Nguyen *et al.*, 1995). The phenomenon of strain diversity among TSE diseases is thought to result from variations in beta sheet conformation by the particular strain (Willie *et al.*, 2002; Ma and Lindquist, 2002).

The entire polypeptide of 231 amino acids contain residues 1 – 23 as signal peptide from the amino terminal followed by the more important octa-repeat region PHGGGWGQ repeated four times and responsible for cooperatively binding four copper ions and spanning residues 60 – 91. A fifth copper

binding site has also been located within residues 90 – 115, by coordination of His96 and His111 (Cereghetti *et al.*, 2001, Hasnain, 2001). Considerable effort has been made to study copper binding to the amino terminal octarepeat region. Circular dichroism (CD), electron paramagnetic resonance (EPR) and crystallographic studies have all been used to access the binding of copper, the flexibility and structure of this region. The dissociation constants for copper binding are known to be between 1nM and 10uM even in the femtomolar range. However, the binding of copper at the fifth site located by the carboxyl terminal region of PrP is poorly understood and is still to be assessed. Although the greater interest of copper binding at the N-terminal octa-repeats has contributed to the elucidation of PrP<sup>C</sup> as an important factor in metal ion regulation (Hornshaw *et al.*, 1995) against oxidative stress (Tobler *et al.*, 1996), studies with transgenic mice lacking the octa-repeats indicate that these mice were still susceptible to infection, suggesting that the N-terminal octa-repeats were not necessary for infectivity. In contrast, studies with radioactive copper at physiological concentrations showed a significant reduction of copper binding in prion infected cells (Waggoner *et al.*, 2000; Brown *et al.*, 2001; 2002). This observation does not rule out a role for copper in initiating TSE infection when its concentration has exceeded tolerant levels for different cells. The presence of a fifth site of high copper affinity within the carboxyl terminus is reportedly essential for amyloid formation as well as enhancing infectivity. Thus, there are two structurally different copper binding sites with different affinities: the N-terminal octa-repeats evolutionarily conserved for binding and regulating copper levels in cells, and the carboxyl terminal fifth copper site which not only serves as a copper sensor but also in inducing infectivity in the presence of excess copper which varies between cells. Furthermore, copper binding within the 90 – 231 carboxyl terminal regions is also associated with the increased protease resistance due to changes in secondary structure and the induction of a more structured form. Also PrP residues 106 – 126 in soluble and amyloid clusters are reported to

owe their neurotoxicity to the binding of copper to its fifth site within the carboxyl terminal region (Hornshaw *et al.*, 1995).

While the N-terminal octa-repeats of PrP have been conserved as a sink for metals and scavenger for copper thereby enhancing the anti-oxidant potential of various cells, the C-terminal region which is within the 90 – 231 segment with its three alpha helices and two beta strands may have evolved as a sensor for copper levels, which it is proposed, when it exceeds intolerant levels to the cells may enhance the proteins potential for infectivity or amyloid formation. The investigation on the structure of the various monomeric segments of PrP and their amyloids using recombinant isoforms by visible, infrared spectroscopy and electron microscopy indicated that copper induces conformational similarity of the non-fibrillar 90 – 231 isoform by increasing its beta sheet content and absorbance in the 700nm region which are indistinguishable from its amyloid form. The present study seeks to establish the structural forms of metal induced conformational changes of prion protein into  $\beta$ -sheet isoforms similar to amyloid.

## MATERIALS AND METHODS

**UV-Visible Spectroscopy:** An OLIS conversion of a Cary 16 UV/visible spectrophotometer was used to collect spectra. 100ul of 0.2mg/ml of recombinant protein were used except for 263K where the final concentration was 5uM. For the metals, copper and zinc were obtained as 1M stock of copper sulfate and zinc acetate and in all cases 100ul of 10uM of either zinc or copper was used. The solutions were made up in 1% PBS buffer which also served as base line to generate the spectra. For the pH experiment, the pH were adjusted from 4 to 9 with 100ul of 1M stock of sodium acetate trihydrate, sodium citrate dehydrate, sodium cacodylate, sodium HEPES, Tris hydrochloride, and 0.5M CAPSO all purchased from Hampton Research. Protein concentrations were determined using BCA protein assay kit.

**Purification of Recombinant Prion Protein:** Hamster and mouse prion protein peptides were

purified with modifications to the method of Zahn *et al.* (1997; 2000). Prion protein (PrP) sequences (corresponding to residues 23 – 144, 90 – 231 or 23 – 231) were amplified by PCR, ligated into the pET41 vector (EMD Biosciences) as NdeI/HindIII inserts and the constructs were verified by DNA sequencing. Plasmids were then transformed into *E. coli*. Rosetta cells (EMD Biosciences) and expressed in the form of inclusion bodies with the overnight express auto induction system (EMD Biosciences). Harvested cell pellets were lysed with 30mL BugBuster<sup>®</sup>/60mL lysonase (EMD Biosciences) per 1 gram cell pellet in the presence of EDTA-free protease inhibitors (Roche). Inclusion bodies were further washed with 0.1X BugBuster<sup>®</sup>, and then suspended in 6M Guanidine hydrochloride, 100mM phosphate, 10mM Tris, pH 8. Cell debris was pelleted by centrifugation and the supernatant was stirred with NiNTA super flow resin (Qiagen) and loaded into an XK16/20 column. A linear gradient was run with an AKTA liquid chromatograph system over 6 hr into refolding buffer (100mM phosphate, 10mM Tris, pH 8). The protein was eluted with 100 mM sodium phosphate (pH 5.8), 500 mM imidazole, 10 mM Tris. Pooled fractions were exhaustively dialyzed against 10 mM phosphate at pH 5.8. Purity of the final protein preparations was estimated at 99% when analyzed by SDS-PAGE.

**Fibrillization of Recombinant Prion Protein:** Full-length hamster and mouse rPrP were concentrated by centrifugal ultra filtration (Amicon) to 1.2mg/mL and agitated in fibrillization buffer (500mM Guanidine hydrochloride, 1.2M urea 25mM phosphate, pH 6.5) at 1,000rpm for 24 hr. Solid material was isolated by centrifugation and washed twice with water. The pelleted material was composed primarily of amyloid-like fibrillar material, as evidenced by transmission electron microscopy (see below). For experimental purposes, the water-washed pelleted fibrillar material was suspended in the buffer of choice and diluted to the appropriate concentration, as specified for each experiment.

**Transmission Electron Microscopy:** Aqueous samples of fibrillar material were diluted to - 50mg/mL with water and briefly sonicated to effect homogeneity. Sample suspensions (5mL) were settled on formvar coated copper grids. Excess fluids were micropipetted from the grid surface, washed with water, and stained for 60 seconds with 0.3% aqueous uranyl acetate. Excess stain was removed and the samples dried at room temperature. The samples were analyzed at 80kV in a Hitachi 7500 electron microscope or 60 kV on a Philips CM-10 (FE1, Hillsboro, OR) transmission electron microscope. Digital images were captured with an AMT digital camera system (AMT, Chazy, NY).

## RESULTS

### Characterization of Purified PrPsc/rec PrP by SDS-PAGE Electrophoresis, Electron Microscopy and UV-Visible Spectroscopy:

The purified recombinant prion protein segments (Figure 1a) had lane 1 represented by the marker, while lane 2 to 5 had the purified prion fragments on the basis of their molecular weights, lane 2 and 3 showed the human recombinant prion (recHu- prp 23 – 231) which had a similar molecular weight to that of mouse (rec MoPrP 23 – 231). Lanes 4 and 5 represents the smaller PrP segments: rec MoPrP 90 – 231, and rec. Ha PrP 23-144 (145 stop). Also the electron micrographs of each of the recombinant non-fibrillar rPrP-Sen are shown with their respective amyloid structure (Figure 1b).

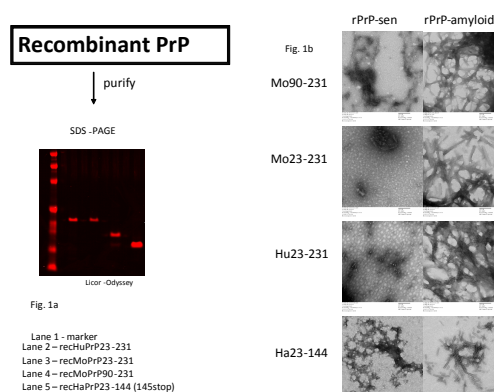


**Figure 1 : The purified recombinant prion protein segments**

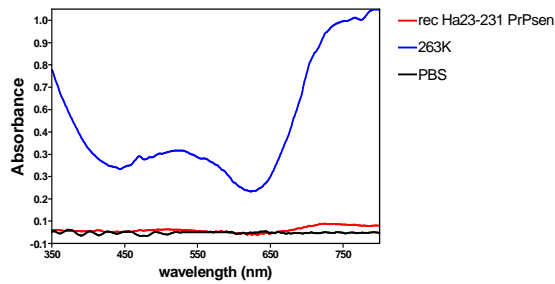


**Figure 2: The UV-visible spectrum of Hamster adapted scrapie (263K) in PBS.**

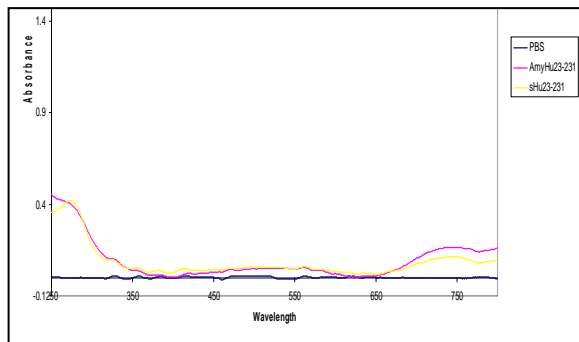


**Figure 3a: Non-fibrillized recombinant PrP isoforms**

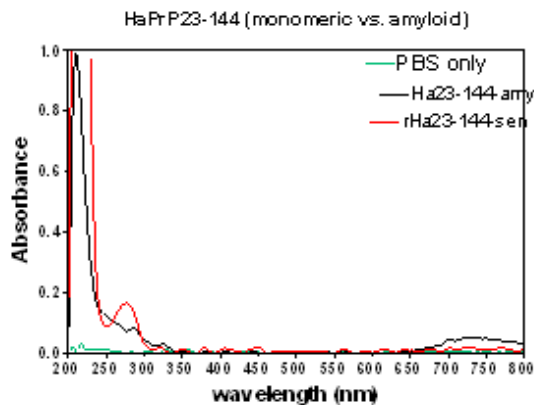


**Figure 3b: Non-fibrillized recombinant PrP isoforms**

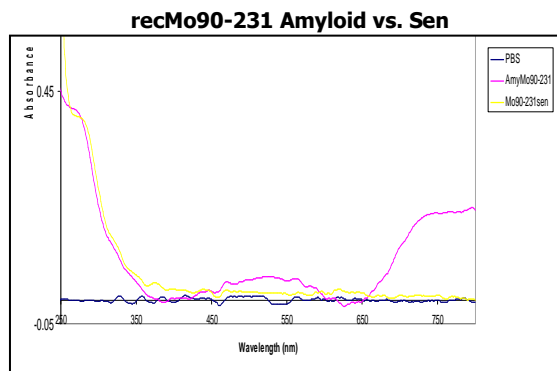


**Figure 3c: Non-fibrillized recombinant PrP isoforms**

In each case the non-fibrillated (rPrP-Sen) Isoforms are smaller and amorphous while the polymeric structures are consistent with the ultra structure of amyloid fibrils. The UV-visible spectrum of Hamster adapted scrapie (263K) in PBS, pH 7.0 exhibited a broad absorbance at 450 – 650 nm which is four times lower in intensity than the corresponding increase in absorption at 750nm (Figure 2). Why does 263K PrP-res exhibit absorbance at 750 nm, when 263K is not necessarily PrP only but ferritin, Fe, Cu etc? This high intensity at 750 nm was markedly reduced or absent in the (non-infectious) non-fibrillized recombinant PrP isoforms (hamster Rec-23-231, human rec23 – 231, mouse 23 – 144) (Figure 3). Especially note worthy is the comparison between the spectra of the non-fibrillar isoforms and amyloid. While slight differences in the 750nm absorbance was observed between the non-fibrillar rec/Hu PrP 23 – 231 rec Ha 23 – 231 and see Ha PrP 23 – 144 segment, and their amyloids a significant increase in absorbance exist between the 90-231 non-fibrillar segment and its amyloid (figure 3c). Also the presence of copper in the 90-231 non-fibrillar segments increases the 750nm absorption to approach that of the 90 – 231 amyloid spectra. The N-terminal (23 – 231) full segment showed no such spectral differences at 750nm absorption with the amyloid (Figure 4).

**Fourier Transform Infrared Spectroscopy:**

A comparison of non-fibrillar versus fibrillar rMoPrP 90-231 indicated a major shift in their infrared spectra between 1700cm<sup>-1</sup> and 1600cm<sup>-1</sup>, the amide I region which is important in the characterization of protein secondary structure. Addition of copper to the non-aggregated Mo90-231 led to a shift similar to the band position of the amyloid isoform (Figure 5).

**DISCUSSION**

This study supported the fact that the capacity of prion proteins to form amyloids might be inherent within the amino acid residues 90 – 231.

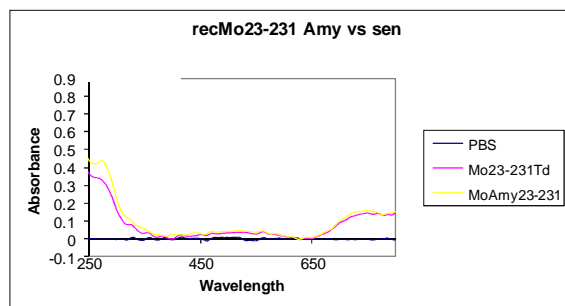


**Figure 4: The N-terminal (23 – 231) full segment with no spectral differences at 750nm absorption.**

**FTIR: recMo90-231 with  $\text{Cu}^{++}$  prompts formation of  $\beta$ -sheet**

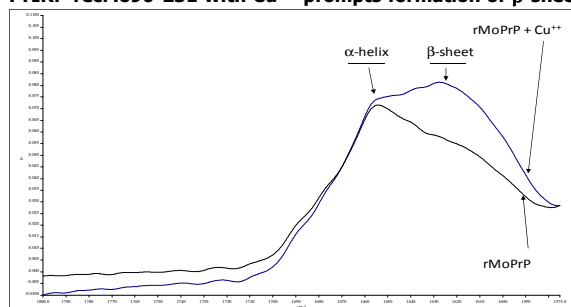


**Figure 5: Addition of copper to the non-aggregated Mo90-231 indicated by a shift similar to the band position of the amyloid isoform**

Our UV-visible spectra which shows a markedly enhanced broad absorbance at the 740 – 750nm region for the amyloid structure of recPrP 90 – 231 is similar to the unusually high absorbance observed for the proteinase K resistant and infectious scrapie form (263K) (Figure 2), and comparison of the absorbance changes between the various prion amyloids and their respective monomeric isoforms (23 – 231, 23 – 144, 90 – 231) within the 740 – 750 nm region indicated a most pronounced difference for the 90 – 231 segment (Figure 4). The full length isoforms (23 – 231) and the 23 – 144 segment did not present major absorbance differences with their respective amyloids that was comparable with the marked difference observed for the non-fibrillar 90 – 231 segment and its amyloid (Hornshaw *et al.*, 1995). More surprising was the small absorbance difference between the non-fibrillar isoform of the 23 – 144 segments and its amyloid with its strong tendency to form stable fibrillar amyloids.

Since the full length (23 – 231), and the 23 – 144 isoforms contain the N-terminal amino acid residues which include the octa-repeats

known to bind and transport copper, exhibited relatively very little differences in absorbance with their amyloid forms at the 740 – 750nm region, the increase in absorbance of the non-fibrillar forms may be due to the interference of copper that were still bound to their-N-terminals. The 90 – 231 non-fibrillar segment on the other hand, lacking the N-terminal octa-repeats does not have such N-terminal copper and therefore has a markedly reduced absorbance at the 740 – 750 nm region, and greater difference in absorbance with its amyloid isoform. Also this increased difference in absorbance between the non-fibrillar 90 – 231 isoform with its amyloid indicated that the capacity to form amyloids was within the carboxyl terminal amino acid residues than the N-terminal residues, containing the octa-repeats. A similar interpretation is that some level of aggregation of the monomeric isoforms already has occurred in the full length (23 – 231) and 23 – 144 non-fibrillar segments which is absent in the non-fibrillar 90 – 231 segment, due to its lack of the N-terminal amino acid residues involving the octa-repeats and the binding of copper. However, complete fibrillation and formation of amyloid under favourable conditions require the presence of amino acids within the 90 – 231 carboxyl terminal residues. Perhaps the presence of copper at its N-terminal octarepeat site where it binds with a lower affinity may initiate some fibrillation in the full length and 23 – 144 non-fibrillar isoforms which may in part explain the relatively little differences in their absorbance spectra at 740 – 750 nm with their amyloids, compared to the 90 – 231 segment where a major change in absorbance exist with its amyloid form (Hornshaw *et al.*, 1995).

Furthermore, figure 5 showed the infrared spectra of the non fibrillar 90 – 231 segment and its amyloid isoform which indicates the higher alpha helical content of the non-fibrillar segment compared to the amyloid spectrum which shows its higher beta sheet content. Addition of copper to the non-fibrillar isoform causes a shift in its spectrum making it similar to the high beta sheet amyloid isoform, supporting the consideration of copper binding to the residues within the 90 – 231 non-fibrillar

segment of PrP as essential for the formation of amyloid. It is puzzling that the same non-fibrillar recombinant PrP isoform was used to generate their respective amyloids, yet the presence of copper in the 90 – 231 segment yielded amyloid that gave an increased UV Visible absorbance at 740 – 750nm region supported by an increased beta sheet structure, while its non-fibrillar isoform gave no such absorbance and no such change in its secondary structure, unless exogenous copper was added which induced a change to higher absorbance and higher beta sheet structure similar to the amyloid. Perhaps the site for copper binding on the non-fibrillar isoform of the 90 – 231 segment which has been implicated to involve His 111 and or His 96 is not accessible to copper in its monomeric state, but becomes accessible only in the amyloid state determined by a critical number of aggregated fibrils of this isoform, which among other processes remain to be shown. This complex may constitute the initial nucleation event in the transition from the non-fibrillar structure to the amyloid which triggers the structural changes that include the enhanced beta-sheet structure in the copper induced absorbance at the 740 – 750nm region evident in the amyloid isoforms.

## REFERENCES

- BORCHELT, D. R., ROGERS, M., STAHL, N., TELLING G. and PRUSINER S. B. (1993). Release of cellular prion protein from cultured cells after loss of its GPI anchor. *Glycobiology*, 3: 319 – 329.
- BROWN, D. R., NICHOLAS, R. S. J. and CABEVARI. L. (2002). Lack of prion problem expression results in neuronal phenotype sensitive to stress. *Journal of Neuroscience Research*, 67: 211 – 224.
- BROWN, D. R., CLIVE, C. and HASWELL, S. J. (2001). Antioxidant activity related to copper binding of nature prion protein. *Journal of Neurochemistry*, 76: 69 – 76.
- CALLAHAN, M. A., XIONG, L. and CAUGHEY, B. (2001). Reversibility of scrapie associated prion protein aggregation. *Journal of Biological Chemistry*, 276: 28022 – 28028.
- MA, J. and LINQUIST, S. (2002). Conversion of PrP to a self-perpetuating PrP-Sc like conformation in the cytosol. *Science*, 298: 1785 – 1788.
- CEREGHETTI, G. M., SCHWEIGER, A., GLOCKSHUBER, R. and VAN DOORSLAER, S. (2001). Electron paramagnetic evidence for binding of Cu<sup>2+</sup> to C-terminal domain of the murine prion protein *Biophysics Journal*, 81: 516 – 525.
- HASNAIN, S. S., MURPHY, L. M., STRANGE, R., W., GROSSMAN, J. C., CLARKE, A. R., JACKSON, G. S. and COLLINGE, J. (2001). XAFS study of the high affinity copper binding site of human PrP 90 – 231 and its low resolution structure in solution. *Journal of Molecular Biology*, 311: 467 – 473.
- HORNSHAW, M. P., MCDERMOTT, J. R. and CANDLY, J. M. (1995). Copper binding to the N-terminal tandem repeat regions of mammalian and avian prion protein *Biochemistry and Biophysics Research Communications*, 207: 621 – 629.
- NGUYEN, J. T., INOUE, H., BALDWIN, M. A., FLOTTERICK, R. J., COHEN, F. E., PRUSINER, S. B. and KIRSCHNER, D. A. (1995). X-ray diffraction of scrapie prion rods and PrP Peptides. *Journal of Molecular Biology*, 252: 412 – 422.
- TOBLER, I., GAUS, S. E., DEBOER, T., ACHERMANN, P., FISHER, M., RULICKE, T., MOSER, M., OESH, B., MCBRIDE, P. A. and MANSO, J. C. (1996). Altered Circadian rhythms and sleep in mouse devoid of prion proteins. *Nature*, 380: 639 – 642.
- WAGGONER, D. J., DRISALDI, B., BARTNIKAS, T. B., CASARENO, R. C., PROHASKA, B., GITIN, J. R. and HARIS, J. D. (2000). Brain copper content and cuproenzyme activity does not vary with prion protein expression level. *Journal of Biological Chemistry*, 275: 7455 – 7458.
- WILLIAMS, E. S. and MILLER, M. W. (2002). Chronic wasting disease in deer and Elk in North America. *Revue Scientifique et Technique*, 21: 305 – 316.

- WILLIE, H., MICHELITSCH, M. D., GUENEBAUT, V., SUPATTAPONE, S., SERBAN, A., COHEN, F. E., AGARD, D. A. and PRUSINER, S. B. (2002). Structural studies of the scrapie prion problem by electron crystallography PNAS, 99: 3563 – 3568.
- ZAHN R, VON SCHROETTER, C. and WÜTHRICH, K. (1997). Human prion proteins expressed in *Escherichia coli* and purified by high-affinity column refolding. *Federation of Europeans Biochemical Societies Letters*, 417(3): 400 – 404.
- ZAHN, R., LIU, A., LUEHRS, T., RIEK, R., VON SCHROETTER, C., GARCIA, F. L., BILLETER, M., CALZOLAI, L., WIDER, G. and WÜTHRICH, K. (2000). NMR solution structure of the human prion protein. *Proceeding of National Academy of Sciences*, 97: 145 – 150.